

# RADIATION EFFECTS ON PERFORMANCES OF RADIATIVE GAS HEAT EXCHANGERS AT HIGH TEMPERATURES

Y. MORI, Y. YAMADA\* and K. HIJIKATA

Department of Physical Engineering, Tokyo Institute of Technology, Ohokayama 2-12,  
 Meguro-ku, Tokyo 152, Japan

(Received 18 May 1978)

**Abstract**—Working fluids in heat exchangers of the application system in a High Temperature Gas-Cooled Reactor (HTGR) are considered as radiative gases such as steam, CO and so on. In this paper, radiation effects on performances of heat exchangers which heat up radiative gas such as steam by high temperature helium are theoretically studied. A method to obtain approximate solutions is proposed to be applicable to many practical problems in wide ranges of temperature, pressure, gas absorptivity and so on. Then heat transfer performances of constant heat flux case for one duct and case of counterflow heat exchangers with two ducts are calculated to give fundamental information on heat exchangers of hot helium and steam.

## NOMENCLATURE

$a$ , width of flow duct [m];  
 $C_p$ , specific heat at constant pressure [ $\text{J kg}^{-1} \text{K}^{-1}$ ];  
 $E_n$ , attenuation function of one-dimensional radiation;  
 $h$ , heat-transfer coefficient [ $\text{W m}^{-2} \text{K}^{-1}$ ];  
 $l$ , length of flow duct [m for dimensional value];  
 $M$ , radiation-convection parameter,  $\equiv \varepsilon \sigma \bar{T}_0^3 / h$ ;  
 $N$ , radiation conduction parameter,  $\equiv 2a\sigma \bar{T}_0^3 / \lambda$ ;  
 $Nu$ , Nusselt number,  $\equiv 2ah / \lambda$ ;  
 $Pr$ , Prandtl number,  $\equiv \mu C_p / \lambda$ ;  
 $Q$ , heat flux on the wall [ $\text{W m}^{-2}$  for dimensional value];  
 $\bar{q}$ , heat flux other than radiation [ $\text{W m}^{-2}$ ];  
 $\bar{q}_R$ , radiative heat flux [ $\text{W m}^{-2}$ ];  
 $Re$ , Reynolds number,  $\equiv 2a\rho \bar{U}_m / \mu$ ;  
 $St$ , Stanton number,  $\equiv Nu / (RePr) \equiv h / \rho C_p \bar{U}_m$ ;  
 $T_g$ , temperature of the fluid [K for dimensional value];  
 $T_m$ , mixed mean temperature [K for dimensional value];  
 $T_r$ , radiative mean temperature [K for dimensional value];  
 $T_w$ , wall temperature [K for dimensional value];  
 $t$ , optical thickness;  
 $U$ , flow velocity [ $\text{m s}^{-1}$  for dimensional value];  
 $U_m$ , mean flow velocity [ $\text{m s}^{-1}$  for dimensional value];  
 $x$ , co-ordinate in flow direction [m for dimensional value];  
 $y, z$ , co-ordinates vertical to flow direction [m for dimensional value].

$\kappa$ , absorptivity [ $\text{m}^{-1}$ ];  
 $\lambda$ , thermal conductivity [ $\text{W m}^{-1} \text{K}^{-1}$ ];  
 $\mu$ , viscosity [ $\text{Pa s}$ ];  
 $\nu$ , kinematic viscosity [ $\text{m}^2 \text{s}^{-1}$ ];  
 $\rho$ , density [ $\text{kg m}^{-3}$ ];  
 $\sigma$ , Stefan Boltzmann constant [ $\text{W m}^{-2} \text{K}^{-4}$ ];  
 $\tau$ , optical thickness,  $= \kappa \bar{y}$ ;  
 $\phi$ , non-dimensional heat flux,  $= QNu/2$ .

## Subscripts

$d$ , optical thickness of flow duct width;  
 $i$ , fluid (1 or 2);  
 $j$ , wall (1, 2 or 3);  
 $ij$ , wall  $j$  in contact with fluid  $i$ ;  
 $0$ , inlet of low temperature side;  
 $1$ , low temperature wall or fluid;  
 $2$ , high temperature wall or fluid;  
 $3$ , intermediate wall;  
 $—$ , dimensional value (to be only applicable when denoted as for dimensional value).

## 1. INTRODUCTION

THE HIGH temperature helium gas-cooled reactor has not only a potential to be used in various fields for an effective use of its nuclear energy, but also has a better safety performance compared with the conventional water-cooled nuclear reactor. The effective use of nuclear energy is promising when the working fluid comes out at a high temperature (about  $1000^\circ\text{C}$ ) from the reactor core, the potential of which shows prospects for multi-purpose cascade use such as direct steel-making by use of high temperature hydrogen, industrial use of naphtha field and hydrogen manufacture and electric power generation by helium or steam turbine. From the viewpoint of reactor safety, as the neutron collective cross section of helium is small and the fuel is covered with multiple carbon layers, the amount of radiation waste is extremely small compared with those from other type of reactors e.g. light

## Greek symbols

$\varepsilon$ , emissivity of wall;  
 $\varepsilon_H$ , eddy thermal diffusivity [ $\text{m}^2 \text{s}^{-1}$ ];

\* Mechanical Engineering Laboratory, Agency of Industrial Science and Technology, Tsakuba, Ibaraki, Japan.

water reactors. Moreover, as the working temperature is high, thermal pollution caused by warm exhaust water could be reduced. Furthermore, this high temperature gas-cooled reactor could be considered to give technical fundamentals in the development of a gas-cooled fast breeder reactor or gas-cooling of blanket of a fusion reactor.

Helium can be reasonably selected as the working fluid for the high temperature reactor. Helium itself is non-radiating in the temperature region of about 1000°C. In this case, radiation from the reactor wall and the heat exchanger wall at high temperature gives a big augmentation effect on heat transfer performances of the reactor core and heat exchangers. A theoretical calculation has already been reported in our previous report [1] on radiation effects on performances of heat exchangers when the working fluid is a non-radiating gas such as helium and experimental results to prove theoretical predictions have been reported previously [2].

On the other hand, if the high temperature gas reactor is used for electrical power generation and multi-purposes, as the thermal energy generated in the reactor core operates the steam generator and the steam reformer and so on in the first and the second loops, the steam which is a radiating gas is required to be heated up to a high temperature. For such heat exchanges of radiating gases, theoretical calculations and experiments made for limited cases have been reported [3–6]. In these calculations, the following simplified cases are treated: A grey radiating gas is flowing between the black parallel walls under isothermal [3,5,6], or constant heat flux conditions [4], and the energy equation in the gas is numerically solved, and heat transfer performance is discussed from the temperature distribution of gas in a cross section obtained from numerical calculations. However, for the practical heat exchangers, the assumption of emissivities of walls to be unity and the condition of the wall temperatures and the heat fluxes of both sides being equally constant, are not reasonable. In the case of a very turbulent flow or two-ducts, calculations will be very complicated and difficult using the calculation methods reported so far.

In our present report, a high temperature heat exchanger for heating up steam by helium from the high temperature gas reactor was modeled, and considering the case of radiating gas flowing between the parallel flat plates, theoretical analyses were made in the cases of the constant heat flux in one duct and the counter flow heat exchanger of two ducts, to make clear radiation effects on heat transfer performances in laminar and turbulent regions.

## 2. FUNDAMENTAL EQUATIONS

As the model for an analysis, a two dimensional case is considered when fluids flow in the two ducts with parallel walls separated by an intermediate wall as shown in Fig. 1. The following assumptions are made, (1) The working fluids are grey radiating gases of

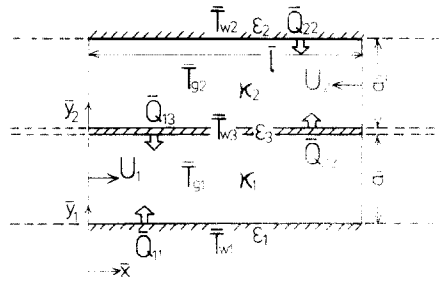


FIG. 1. Physical model and co-ordinate system.

absorptivities  $\kappa_1$ ,  $\kappa_2$  and the solid walls are grey of emissivities  $\epsilon_1$ ,  $\epsilon_2$ ,  $\epsilon_3$  and are of diffuse reflection. (2) Radiation is assumed to be one-dimensional. This means that when heat balance at point  $\bar{x}$  is considered, calculations for radiative heat flux are made on the assumption that the temperature distribution in the cross section at the  $\bar{x}$  point is similarly applicable to those at all other  $\bar{x}$  points. This assumption is appropriate in the region where the temperature varies linearly to the  $\bar{x}$  direction, except in the neighbourhoods of the inlet and outlet parts. This assumption has been proved to be adequate by the calculation made under condition of two-dimensional radiation [5]. (3) The forced convection heat transfer coefficients is equal to that without radiation. Hasegawa *et al.* [4] have reported that the Nusselt number of the forced convection flow of radiating gas shows a different value from that without radiation, but the difference is small and will not have a large effect on the results of the present report as explained later. (4) The thermal conduction to the  $\bar{x}$  direction in the solid wall is appropriately neglected.

Under such conditions described above, and shown in Fig. 1 the gas flowing in from the left is of a low temperature and indicated by the subscript 1, the high temperature gas flowing in from the right is indicated by the subscript 2. The heat balance of the low temperature gas is given by equation (1). In equation (1), a distribution to the  $\bar{y}$  direction is not considered, and according to assumption (3) the forced convective heat transfer coefficient  $h$  is used. Subscripts 1, 2 and 3 in relation to the walls are applied in the order of the low temperature, high temperature and intermediate walls, and the subscripts consisting of two letters as  $ij$  express the values at the wall  $j$  in contact with the gas  $i$ . The energy equations of the low temperature and the intermediate walls are expressed by equations (2) and (3).

$$\rho_1 c_{p1} \bar{U}_m a_1 \frac{d\bar{T}_{m1}}{d\bar{x}} = h_{11}(\bar{T}_{w1} - \bar{T}_{m1}) + h_{13}(\bar{T}_{w3} - \bar{T}_{m1}) + \bar{q}_R(0) - \bar{q}_R(\tau_{1d}) \quad (1)$$

$$\sigma \bar{T}_{w1}^4 - \frac{\bar{q}_{11}}{\epsilon_1} = \left( \sigma \bar{T}_{w3}^4 - \frac{1 - \epsilon_3}{\epsilon_3} \bar{q}_{13} \right) 2E_3(\tau_{1d}) + 2\sigma \int_0^{\tau_{1d}} \bar{T}_{g1}^4(\tau_1) E_2(\tau_1) d\tau_1 \quad (2)$$

$$\sigma \bar{T}_{w3}^4 - \frac{\bar{q}_{13}}{\varepsilon_3} = \left( \sigma \bar{T}_{w1}^4 - \frac{1 - \varepsilon_1}{\varepsilon_1} \bar{q}_{11} \right) 2E_3(\tau_{1d}) + 2\sigma \int_0^{\tau_{1d}} \bar{T}_{g1}^4(\tau_1) E_2(\tau_{1d} - \tau_1) d\tau_1. \quad (3)$$

Here  $\bar{T}_{m1}$ ,  $\bar{U}_{m1}$ ,  $\bar{q}_{1j}$ ,  $q_R(0)$ ,  $\bar{q}_R(\tau_{1d})$  indicate the mixed-mean temperature, the mean flow velocity, the heat flux other than radiation (convective heat flux and heat inputs from outside) and the radiative heat fluxes on both side walls, respectively, which are expressed as follows:

$$\bar{T}_{m1} = \int_0^{a_1} \bar{U}_1 \bar{T}_{g1} d\bar{y}_1 / \int_0^{a_1} \bar{U}_1 d\bar{y}_1, \quad (4)$$

$$\bar{U}_{m1} = \int_0^{a_1} \bar{U}_1 d\bar{y}_1 / a_1$$

$$\bar{q}_{1j} = \bar{Q}_{1j} - h_{1j}(\bar{T}_{wj} - \bar{T}_{m1}), \quad j = 1, 3 \quad (5)$$

$$\bar{q}_R(0) = 2 \left[ \left( \sigma \bar{T}_{w1}^4 - \frac{1 - \varepsilon_1}{\varepsilon_1} \bar{q}_{11} \right) E_3(0) - \left( \sigma \bar{T}_{w3}^4 - \frac{1 - \varepsilon_3}{\varepsilon_3} q_{13} \right) E_3(\tau_{1d}) - \sigma \int_0^{\tau_{1d}} \bar{T}_{g1}^4(\tau_1) E_2(\tau_1) d\tau_1 \right]$$

$$\bar{q}_R(\tau_{1d}) = 2 \left[ \left( \sigma \bar{T}_{w1}^4 - \frac{1 - \varepsilon_1}{\varepsilon_1} \bar{q}_{11} \right) E_3(\tau_{1d}) - \left( \sigma \bar{T}_{w3}^4 - \frac{1 - \varepsilon_3}{\varepsilon_3} \bar{q}_{13} \right) E_3(0) + \sigma \int_0^{\tau_{1d}} \bar{T}_{g1}^4(\tau_1) E_2(\tau_{1d} - \tau_1) d\tau_1 \right] \quad (6)$$

where

$$\tau_1 = \kappa_1 \bar{y}_1, \quad \tau_{1d} = \kappa_1 a_1 \quad (7)$$

$$E_n(\tau) = \int_0^1 \mu^{n-2} \exp(-\tau/\mu) d\mu. \quad (8)$$

Equation (2) expresses the heat balance of the low temperature wall and the LHS indicates the emitted radiation, the heat loss and the convective heat to the gas, while the first term of the right-hand side expresses the heat reaching the low temperature wall, radiation from the opposite intermediate wall being partly absorbed by the gas, and the second term is the heat radiated from the gas and reaching the low temperature wall. Equation (3) is likewise introduced considering the heat balance of the intermediate wall facing the low temperature side. The function  $E_n(\tau)$  appearing in equations (2), (3) and (6) is an attenuation function used for the one-dimensional radiation as expressed by equation (8).

After simplifying equation (1) by use of equations (2)–(6), equations (1), (2) and (3) are made non-dimensional as follows based on the length at the flow duct width  $a_1$  and the inlet temperature of the low temperature gas.

$$\frac{dT_{m1}}{dx_1} = S_{i11} Q_{11} + S_{i13} Q_{13} \quad (9)$$

$$T_{w1}^4 - \frac{1}{M_{11}} (Q_{11} - T_{w1} + T_{m1}) = \left[ T_{w3}^4 - \frac{1 - \varepsilon_3}{M_{13}} (Q_{13} - T_{w3} + T_{m1}) \right] 2E_3(\tau_{1d}) + 2 \int_0^{\tau_{1d}} T_{g1}^4(\tau_1) E_2(\tau_1) d\tau_1 \quad (10)$$

$$T_{w3}^4 - \frac{1}{M_{13}} (Q_{13} - T_{w3} + T_{m1}) = \left[ T_{w1}^4 - \frac{1 - \varepsilon_1}{M_{11}} (Q_{11} - T_{w1} + T_{m1}) \right] 2E_3(\tau_{1d}) + 2 \int_0^{\tau_{1d}} T_{g1}^4(\tau_1) E_2(\tau_{1d} - \tau_1) d\tau_1. \quad (11)$$

The boundary condition is,

$$T_{m1}(0) = 1. \quad (12)$$

The non-dimensional variables appearing in equations (9)–(12) are given as follows:

$$x_i = \frac{\bar{x}}{a_i}, \quad y_i = \frac{\bar{y}}{a_i}, \quad T = \frac{\bar{T}}{\bar{T}_0}, \quad l_i = \frac{l}{a_i}$$

$$S_{ij} = \frac{h_{ij}}{\rho_i c_{pi} U_{mi}} = \frac{Nu_{ij}}{Re_i Pr_i}$$

$$M_{ij} = \frac{\varepsilon_j \sigma \bar{T}_0^3}{h_{ij}} = \frac{\varepsilon_j N_i}{Nu_{ij}},$$

$$N_i = \frac{2a_i \sigma \bar{T}_0^3}{\lambda_i}, \quad Q_{ij} = \frac{\bar{Q}_{ij}}{h_{ij} \bar{T}_0},$$

$$T_{m1} = \int_0^1 U_1 T_{g1} dy_1, \quad U_1 = \frac{\bar{U}_1}{\bar{U}_{m1}}. \quad (13)$$

Furthermore, equation (13) expresses the non-dimensional parameters for the low temperature side when the subscript  $i = 1$  and for the high temperature side when subscript  $i = 2$ .

By giving the heat input from outside and the emissivities of the walls, the parameters  $S_{ij}$ ,  $M_{ij}$ ,  $\varepsilon_j$  and  $Q_{ij}$  in equations (9)–(11) are fixed. The unknown quantities are  $T_{m1}$ ,  $T_{w1}$ ,  $T_{w3}$  and the distribution  $T_{g1}(y_1)$ .  $T_{m1}$ ,  $T_{w1}$  and  $T_{w3}$  cannot be obtained from equations (9)–(11) unless the temperature distribution  $T_{g1}(y_1)$  to the  $y_1$  direction is not given. Therefore, a reference temperature  $T_r$  in a cross section in connection with radiation is defined as follows:

$$T_{r11}^4 = \int_0^{\tau_{1d}} T_{g1}^4(\tau_1) E_2(\tau_1) d\tau_1 / \int_0^{\tau_{1d}} E_2(\tau_1) d\tau_1 \quad (14)$$

$$T_{r13}^4 = \int_0^{\tau_{1d}} T_{g1}^4(\tau_1) E_2(\tau_{1d} - \tau_1) d\tau_1 / \int_0^{\tau_{1d}} E_2(\tau_{1d} - \tau_1) d\tau_1. \quad (15)$$

The relation between this reference temperature (or

radiation mean temperature)  $T_r$  and the mixed-mean temperature  $T_m$  is assumed as follows:

$$T_r = (1 + C)T_m. \quad (16)$$

The coefficient  $C$  is a complicated function of  $T_m$ ,  $T_w$ ,  $\tau_a$  and other parameters. By introducing the mean temperature of radiation  $T_r$  in the same way about the high temperature side, the fundamental equations for the counter flow heat exchanger are as follows from equations (9)–(11).

$$\frac{dT_{mi}}{dx_i} = (-1)^{i+1}(S_{ij}Q_{ij} + S_{is}Q_{is}) \quad (i = j = 1, 2) \quad (17)$$

$$\begin{aligned} T_{wj}^4 - \frac{1}{M_{ij}}(Q_{ij} - T_{wj} + T_{mi}) \\ = \left[ T_{wk}^4 - \frac{1 - \epsilon_k}{M_{ik}}(Q_{ik} - T_{wk} + T_{mi}) \right] \\ \times 2E_3(\tau_{id}) + 2\{1 - E_3(\tau_{id})\}T_{rij}^4. \end{aligned} \quad (18)$$

In equation (18), the subscript  $k$  expresses the quantity about the wall opposite to the wall  $j$  through the fluid, and the combinations of  $i, j$  and  $k$  are given as

$$(i, j, k) = (1, 1, 3), (1, 3, 1), (2, 2, 3), (2, 3, 2). \quad (19)$$

The boundary conditions for the gases are,

$$T_{m1}(0) = 1, \quad T_{m2}(l_2) = 1 + \Delta T. \quad (20)$$

The balance of the heat flux through the intermediate wall is,

$$\left. \frac{Q_{13}}{M_{13}} \right|_{x_1 = x/a_1} + \left. \frac{Q_{23}}{M_{23}} \right|_{x_2 = x/a_2} = 0 \quad (21)$$

Assuming that the value of  $C$  in equation (16) is known beforehand, by using equation (16) equations (17) and (18) will construct a necessary and sufficient equation system for  $T_{mi}$ ,  $T_{wj}$  and  $Q_{i3}$  under the conditions of equations (20) and (21). Thus for the inlet conditions of the high and low temperature gases, temperature and intermediate wall heat flux distributions can be obtained.

### 3. APPROXIMATION SOLUTION

In the beginning it is desirable to investigate the coefficient  $C$  introduced in the preceding section, and for this purpose the energy equation of the gas taking the  $y$  direction variation into consideration should be analysed to find temperature distributions in the gas. A one-dimensional radiation approximation being considered, energy equation of gas for the low temperature side corresponding to equations (1)–(3) is as follows:

$$\begin{aligned} \rho_1 c_{p1} \bar{U}_1 \frac{\partial \bar{T}_{g1}}{\partial x} = \rho_1 c_{p1} \frac{\partial}{\partial y_1} \left[ \left( \frac{v_1}{Pr_1} + \epsilon_H \right) \frac{\partial \bar{T}_{g1}}{\partial y_1} \right] \\ - 2\pi\kappa_1 \left[ \frac{2}{\pi} \sigma \bar{T}_{g1}^4 - \int_0^{\tau_a} \frac{1}{\pi} \right. \\ \left. \times \sigma \bar{T}_{g1}^4 E_1(|\tau_1 - t_1|) dt_1 - I(0)E_2(\tau_1) \right. \end{aligned}$$

$$\left. - I(\tau_{1d})E_2(\tau_{1d} - \tau_1) \right]. \quad (22)$$

Here,  $I(0)$  and  $I(\tau_{1d})$  are given by equations (23) and (24):

$$\begin{aligned} \pi I(0) = \epsilon_1 \sigma \bar{T}_{w1}^4 + 2(1 - \epsilon_1) \left[ \pi I(\tau_{1d})E_3(\tau_{1d}) \right. \\ \left. + \int_0^{\tau_{1d}} \sigma \bar{T}_{g1}^4 E_2(t_1) dt_1 \right] \end{aligned} \quad (23)$$

$$\begin{aligned} \pi I(\tau_{1d}) = \epsilon_3 \sigma \bar{T}_{w3}^4 + 2(1 - \epsilon_3) \left[ \pi I(0)E_3(\tau_{1d}) \right. \\ \left. + \int_0^{\tau_{1d}} \sigma \bar{T}_{g1}^4 E_2(\tau_{1d} - t_1) dt_1 \right] \end{aligned} \quad (24)$$

$\epsilon_H$  is the diffusivity and is zero for the laminar flow. Equation (22) is applicable to cases of the wall emissivities of below 1, and of laminar and turbulent flows. From equation (22), the distribution of  $\bar{T}_{g1}$  to the  $\bar{y}_1$  direction can be determined and thus the value of  $C$  can be calculated from equation (6). The value of  $C$  varies according to the thermal conditions, emissivities and such, but it can be supposed to be a sufficiently smaller value compared with unity. Here we try to determine the value of  $C$ . Hasegawa *et al.* [4] have made numerical calculations for the laminar flow when the emissivities of both walls are unity and the heat fluxes at both walls are equal, the results of which will be compared with our result obtained in the following analysis. For the case of thermal condition on the walls other than those investigated here, the result can be obtained in the same way. In discussing the value of  $C$  the subscripts to express the low temperature gas, the low temperature wall, the intermediate wall etc. will be omitted.

As  $\epsilon = 1$ , equation (23) and (24) are expressed in such a simple form as follows:

$$\pi I(0) = \sigma \bar{T}_w^4, \quad \pi I(\tau_{1d}) = \sigma \bar{T}_w^4. \quad (25)$$

Furthermore, sliding the  $x$ -axis one half to the  $y$ -direction and introducing a  $z$ -axis given by  $z = y - \frac{1}{2}$ , equation (22) is transformed into the following equation.

$$\begin{aligned} \frac{RePr}{2} U \frac{\partial T_g}{\partial x} = \frac{\partial}{\partial z} \left[ \left( 1 + Pr \frac{\epsilon_H}{v} \right) \frac{\partial T_g}{\partial z} \right] \\ - N\tau_d \left[ 2T_g^4 - \int_0^{\tau_d} T_g^4 E_1(|\tau - t|) dt \right. \\ \left. - T_w^4 E_2(\tau) - T_w^4 E_2(\tau_d - \tau) \right]. \end{aligned} \quad (26)$$

To eliminate singularity at  $t = 0$  of  $E_1(t)$ , partial integration is performed to reduce equation (26) to

$$\begin{aligned} \frac{RePr}{2} U \frac{\partial T_g}{\partial x} = \frac{\partial}{\partial z} \left[ \left( 1 + Pr \frac{\epsilon_H}{v} \right) \frac{\partial T_g}{\partial z} \right] \\ - 4N\tau_d \left[ \int_{-1/2}^z E_2(\tau_d(z - z_0)) T_g^3 \frac{\partial T_g}{\partial z_0} dz_0 \right. \end{aligned}$$

$$- \int_z^{1/2} E_2\{\tau_d(z_0 - z)\} T_g^3 \frac{\partial T_g}{\partial z_0} dz_0. \quad (27)$$

On the other hand, from energy equation (10) for the wall,

$$\{1 - 2E_3(\tau_d)\} T_w^4 + \frac{1}{M}(T_w - T_m + Q) = \{1 - 2E_3(\tau_d)\} T_r^4. \quad (28)$$

As the case of the constant heat flux on the wall is considered,

$$\frac{\bar{Q}}{\rho c_p \bar{U}_m \bar{T}_0} = S_i Q = \text{constant}. \quad (29)$$

Assuming that the velocity field has been fully developed and not been affected by the temperature field, it may be given as follows for the laminar and turbulent flows.

$$U = 6\left(\frac{1}{4} - z^2\right): \text{ laminar flow} \quad (30)$$

$$U = \left\{ \begin{array}{l} 0.019775 Re^{3/4} \left(\frac{1}{2} - |z|\right), \quad |z| \leq z_s \\ 1.14265 \left(\frac{1}{2} - |z|\right)^{1/7}, \quad z_s < |z| \leq \frac{1}{2} \\ z_s = \frac{1}{2} - 1.13613 \times 10^2 Re^{-7/8} \end{array} \right\} \quad (31)$$

turbulent flow.

Also  $\varepsilon_H$  is given as,

$$\varepsilon_H = 0: \text{ laminar flow} \quad (32)$$

$$\frac{\varepsilon_H}{v} = \left\{ \begin{array}{l} 5.2801 \times 10^{-2} Re^{7/8} \left(\frac{1}{2} - |z|\right), \quad |z| \leq z_s \\ 0.12131 Re^{3/4} \left(\frac{1}{2} - |z|\right)^{6/7} - 1, \quad z_s \leq |z| \leq \frac{1}{2} \end{array} \right\} \quad (33)$$

turbulent flow.

Solving equation (27) by use of equations (28)–(33), we obtain the temperature distributions in gas and of the walls. However, as equation (27) is a non-linear partial differential integral equation, the exact solution must be made by numerical calculations, and the following approximate solution is obtained in our present report by use of the method of weighted residuals [7].

We assume that the temperature distribution has been fully developed approximately and the following equations may be taken into account:

$$\frac{T_g - T_m}{T_w - T_m} = \theta(z) \quad (34)$$

$$\frac{\partial T_g}{\partial x} = \frac{dT_m}{dx} = \frac{dT_m}{dx} = 2S_i Q. \quad (35)$$

Equation (35) is exactly introduced from equations (34) and (29) when a radiative heat flux is not taken into consideration. When a radiative heat flux exists, equation (35) is also approximately reduced from equation (28) as  $M$  is sufficiently smaller than unity and  $T_r \doteq T_m$ .  $\theta(z)$  in equation (34) is a function of only  $z$ .

$\theta(z)$  is expressed with power series of  $z$ , and is substituted into equation (27) to determine coefficients of power series so as to satisfy equation (27) at the selected points along the  $z$  direction. In consideration of  $\theta(z)$  being symmetrical to the plane of  $z=0$ , it is expressed as follows:

$$\theta(z) = \sum_{n=0}^m \alpha_n z^{2n}. \quad (36)$$

Here  $\alpha_n$  is the unknown coefficient to be determined and  $m$  is the highest exponent of  $z^2$ .

As  $T_g$  is equal to the wall temperature  $T_w$  at the wall, that is,  $z = \pm \frac{1}{2}$ , we have

$$\theta\left(\frac{1}{2}\right) = \sum_{n=0}^m \alpha_n \left(\frac{1}{2}\right)^{2n} = 1. \quad (37)$$

Furthermore, according to the definition of mixed-mean temperature in equation (13), by use of the velocity distribution of equation (30) or equation (31), we get

$$\int_{-1/2}^{1/2} U \theta dz = 0. \quad (38)$$

Equations (37) and (38) are two among  $(m+1)$  equations regarding  $\alpha_n$ . The orthogonal collocation method of the weighted residual is applied to equation (27) for the remaining  $(m-1)$  equations. Substituting equations (35) and (36) into equation (27), the residual is obtained as follows.

$$R(z) = U(z)NuQ - (T_w - T_m) \frac{\partial}{\partial z} \times \left[ \left(1 + Pr \frac{\varepsilon_H(z)}{v}\right) \sum_{n=0}^m 2n\alpha_n z^{2n-1} \right] + 4N\tau_d I(z). \quad (39)$$

Here  $I(z)$  is obtained as follows from the second term of the right-hand side of equation (27):

$$I(z) = \frac{1}{2} \left[ 1 + \frac{\beta\tau_d}{2} + \gamma\tau_d^2 \left( z^2 + \frac{1}{2^2} \right) \right] \times (T_m^4 - T_w^4) + 2T_m^3(T_w - T_m) \times \sum_{n=0}^m \left[ z^{2n} + \frac{\beta\tau_d}{2^{2n+1}(2n+1)} + \frac{\gamma\tau_d^2}{n+1} \left( \frac{z^{2n+2}}{2n+1} + \frac{1}{2^{2n+2}} \right) \right] \alpha_n. \quad (40)$$

To obtain equation (40), the following approximations are used,

$$T_g^4 \doteq T_m^4 + 4T_m^3(T_w - T_m)\theta(z) \quad (41)$$

$$E_2(\tau_d y) \doteq 1 + \beta\tau_d y + \gamma\tau_d^2 y^2 \quad (42)$$

and  $\beta$  and  $\gamma$  are determined as follows from the values of  $E_2(\tau_d y)$  at  $y = \frac{1}{2}$  and  $y = 1$ .

$$\begin{aligned} \log_{10}(-\beta\tau_d) &= 0.251\ 84 + 0.459\ 45 \log \tau_d \\ &\quad - 0.161\ 53(\log \tau_d)^2 \\ \log_{10}(+\gamma\tau_d^2) &= -0.025\ 8 + 0.639\ 45 \log \tau_d \\ &\quad - 0.182\ 72(\log \tau_d)^2 \end{aligned} \tag{43}$$

When  $\theta(z)$  is expressed by the power series of  $z$  up to the extent of  $2m$  power, the residual  $R(z)$  is required to vanish at the selected  $m-1$  points in  $0 \leq z \leq \frac{1}{2}$ . The roots  $z_l (l = 1, 2, \dots, m-1)$  of the orthogonal power series function  $P_{m-1}(z^2) = 0$  are selected for the collocation points taking  $E_2(\tau_d z)$  as the weighting function.

$$\begin{aligned} P_{m-1}(z^2) &= \sum_{k=0}^{m-1} a_k z^{2k}, \\ \int_0^{1/2} E_2(\tau_d z) P_{m-1}(z^2) P_s(z^2) dz &= 0 \end{aligned} \tag{44}$$

$(s = 0, 1, \dots, m-2)$

where  $a_0 = 1, P_0(z^2) = 1$ .

Later, a case of  $m = 2$  is treated, when the selected point  $z_1$  is given as follows:

$$z_1 = \sqrt{\frac{1 + \frac{1}{2}\beta\tau_d + \frac{2}{5}\gamma\tau_d^2}{2^2 \times 3 \left(1 + \frac{1}{2}\beta\tau_d + \frac{1}{3}\gamma\tau_d^2\right)}} \tag{45}$$

This point  $z_1$  approaches the wall as the optical thickness  $\tau_d$  gets larger.

Taking the residual given by equation (39) as zero at the collocation point  $z_l$ , we have

$$R(z_l) = 0 \quad (l = 1, 2, \dots, m-1). \tag{46}$$

Equations (37), (38) and (46) are simultaneous equations for  $\alpha_n$ , but as  $T_w$  has been unknown,  $\alpha_n$  is obtained in a form containing  $T_w$ , by use of which  $T_r$  becomes the following equation.

$$T_r = \left[ 1 + \frac{T_w - T_m}{4T_m} \sum_{n=0}^m \frac{\left\{ (2n+3) \left( 1 + \frac{1}{2}\beta\tau_d \right) + (n+1)\gamma\tau_d^2 \right\} \alpha_n}{(2n+1)(2n+3)2^{2n-2} \left( 1 + \frac{1}{2}\beta\tau_d + \frac{1}{3}\gamma\tau_d^2 \right)} \right] T_m. \tag{47}$$

Here the second term of the big bracket is equal to  $C$  of equation (16). Thus  $T_r$  is obtained as function of  $T_w$  and  $T_m$ .  $T_m$  is given by the following equation (48) from the boundary condition at  $x = 0$ .

$$T_m = 1 + 2S_i Q_x. \tag{48}$$

Introducing equations (47) and (48) to equation (28), and using the following equations in purely forced convection for  $Nu$  of  $M = \epsilon N / Nu$ ,  $T_w$  can be calculated:

$$Nu = 8.235 + \frac{7.2570 \times 10^{-3} (RePr/x)^{1.35}}{1 + 6.135 \times 10^{-3} RePr/x};$$

laminar flow (49)

$$Nu = 0.0356 Re^{0.77} Pr^{0.6} \left( 1 + \frac{0.52610}{\sqrt{0.2}} \right);$$

turbulent flow. (50)

On obtaining  $T_w$ ,  $C$  can be calculated from equation (47).

In the following the numerical results in the case of  $m = 2$  are shown. In Fig. 2, an example is shown of the value of  $C$  obtained in the case of laminar flow. As seen, with an increase of the optical thickness  $\tau_d$ ,  $C$  decreases. This is because of the difference of weighting function of two mean temperatures of  $T_m$  and  $T_r$ . The value of  $C$ , however, is small on the whole and may be reasonably considered below 0.03. The one-dotted chain line in Fig. 3 is the wall temperature plotted for this value of  $C$ , and is compared with the results by Hasegawa *et al.* [4] obtained by numerical calculations shown in a solid line. There exists a small discrepancy when the gas is non-radiative,  $\tau_d = 0$ , which is because of an error in determining the  $Nu$  number in the laminar developing flow, and is not substantial. When  $\tau_d$  is not zero, there also is seen a discrepancy which is not big and the maximum is below 5°C when the standard temperature  $\bar{T}_0$  is 400°C, which may be left out of a practical consideration. Figure 3 also shows in a broken line the wall temperature distributions obtained assuming  $C = 0$  at all the points. There is a difference between the present results and the results of Hasegawa *et al.* but it is small below 10°C, and it is understood that the results obtained assuming  $C = 0$  hold an accuracy of a good enough approximation for practical use.

Figure 4 shows the temperature distributions in gas  $T_g$  obtained in the calculation mentioned above which are plotted with  $x$  as parameter. The broken line is the solution by Hasegawa *et al.* As Hasegawa *et al.* only show temperature distribution at  $x = 5$ , a comparison can be made only with this case; the difference is small, and the accuracy of  $T_g$  by the present calculation is

considered good even at the point of large  $x$ .

Figure 5 shows an example of the value of  $C$  obtained in the case of turbulent flow. There is seen a tendency of decreasing  $C$  in the region of large  $x$  with an increase of  $\tau_d$ . However, in comparison with the case of laminar flow, the value of  $C$  is one order of magnitude smaller, and is below 0.004. This may be because the velocity distribution of turbulent flow is much flatter near the centre than that of the laminar flow. The wall temperature distribution in this case is shown in Fig. 6 and as same in the case of laminar flow the wall temperature decreases with an increase of  $\tau_d$ .

In the present report, about the convective heat

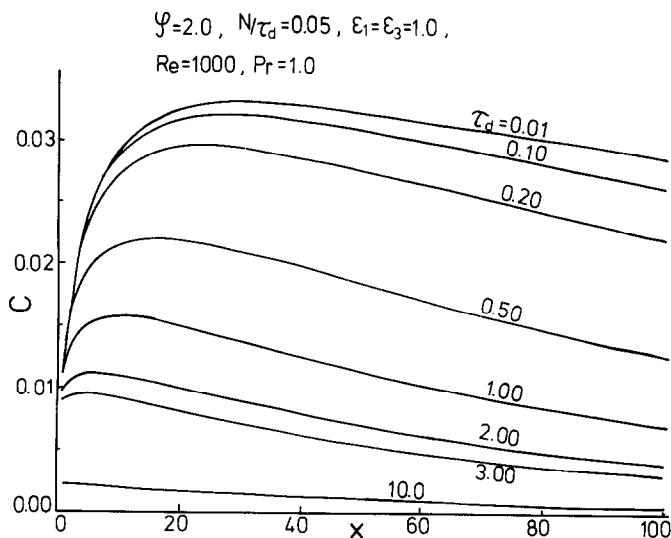


FIG. 2. Value of C in case of laminar flow.

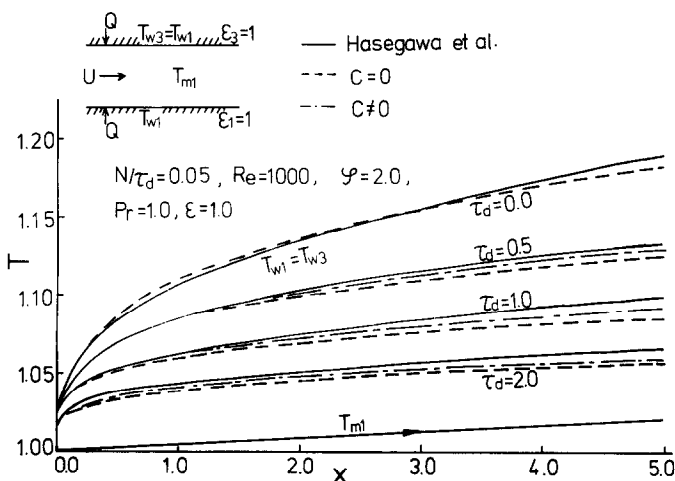


FIG. 3. Comparison of temperature distributions with the results by Hasegawa *et al.* in case of laminar flow.

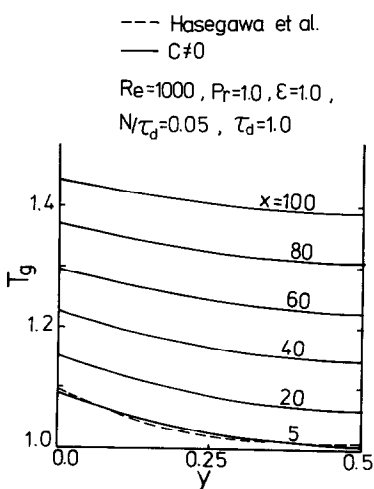


FIG. 4. Temperature profile  $T_g(y)$ .

transfer coefficient, the  $Nu$  number is used purely in the case of convection (equations (49) and (50)). However, as mentioned before with regard to  $C$ , the results of the distributions of  $T_g$  and  $T_w$ , calculated by use of  $Nu$  taking radiation into account, are not much different from those obtained by use of  $Nu$  without radiation effect. This fact has proved the appropriateness of assumption (3).

According to the calculation method mentioned above, the accuracy of the solutions could not be improved only by increasing the number of collocation points, but calculation time may be considerably shorter than that of conventional numerical calculation.

#### 4. RESULTS OF CALCULATIONS

##### 4.1. Constant wall heat flux in the one flow duct

As explained above, the values of  $C$  in equation (16) when heat fluxes from both walls are equal in the flow duct and the emissivities of the walls are unity can be

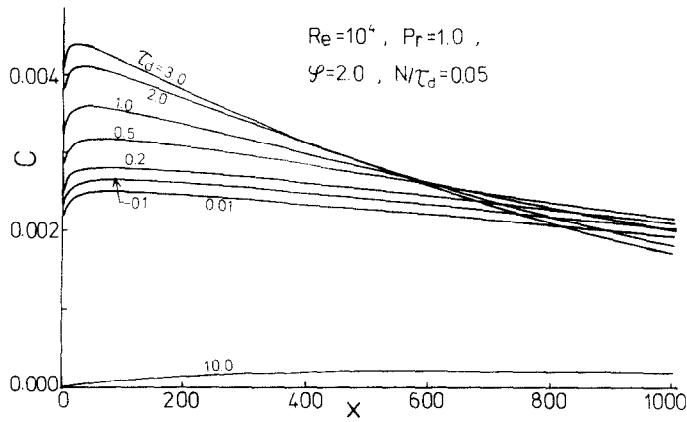


FIG. 5. Value of  $C$  in case of turbulent flow.

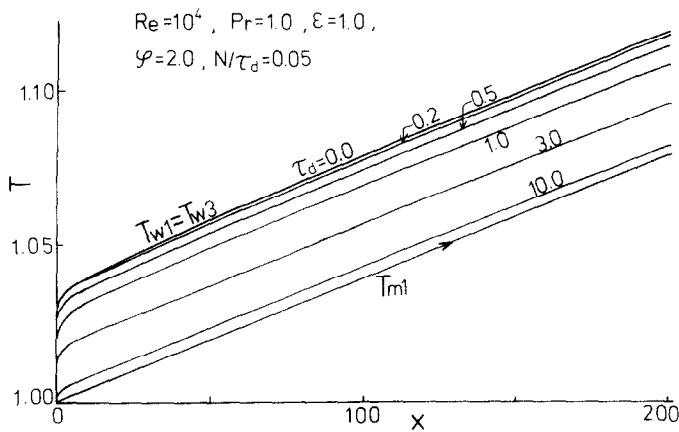


FIG. 6. Temperature distribution in case of turbulent flow.

obtained in good accuracy, and as seen from Figs. 3 and 5, are small compared with unity. In general heat fluxes from both walls are different in one flow duct, and the values of  $C$  on both walls are different. By taking appropriate values for  $C$  and using Figs. 3 and 5, the accuracy of the result is improved, but the purpose of the present report is not to make numerical analyses of all heat exchanger performances. To improve an accuracy of calculation of the performance of a specific heat exchanger, the values of  $C$  can be calculated for the gas and the temperature region to be discussed by use of the method of the present report. In either case, the value of  $C$  is so small compared with unity that it would not cause a large effect, therefore our discussion will proceed in the following numerical calculation with  $C = 0$ .

Figure 7 shows the result of numerical calculation when the heat flux from outside to the wall 3 is constant, the heat flux on the wall 1 is zero and the flow is fully developed laminar. Furthermore the difference of Nusselt numbers  $Nu_{11}$  and  $Nu_{13}$  of both walls due to the difference of the wall temperatures  $T_{w1}$  and  $T_{w3}$  is taken into account by the following equation [8] and iterative calculations are made.

$$Nu_{ij} = \frac{(T_{wk} - T_{mi})\theta^* + T_{wj} - T_{mi}}{(T_{wj} - T_{mi})(1 - \theta^{*2})} Nu^* \quad (51)$$

Here  $Nu^*$  and  $\theta^*$  are given by reference [8], and take, for example, values as follows:

For a fully developed laminar flow:

$$Nu^* = 5.385, \quad \theta^* = 0.346. \quad (52)$$

Furthermore, subscripts  $i, j$  and  $k$  are given by equation (19).

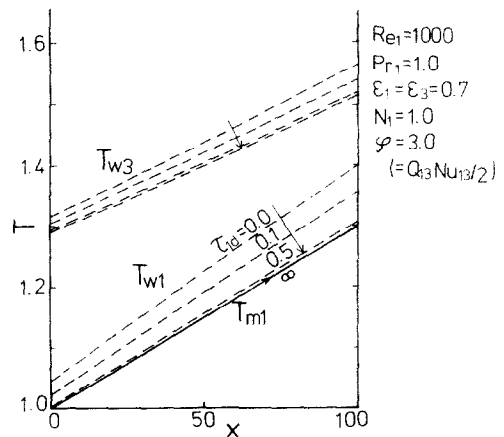


FIG. 7. Case of constant wall heat flux in one flow duct (laminar flow).



As seen from Fig. 7, in the case of  $\tau_d=0$ ,  $T_{w1}$  is much higher than  $T_{m1}$  because radiation from the high temperature wall reaches the low temperature wall. However, with an increase of effect of gas radiation because of increase of  $\tau_d$ , radiation from the high temperature wall is absorbed by the gas on the way. Particularly when  $\tau_d$  is above 2, radiation hardly reaches the low temperature wall, and the temperature of the low temperature wall  $T_{w1}$  becomes equal to the mixed-mean temperature  $T_{m1}$  of the gas. The temperature of the high temperature wall  $T_{w3}$ , decreases as the heat exchange by radiation from the gas becomes active with an increase of  $\tau_d$ , and approaches a constant value when  $\tau_d$  is above 2. Now we take up the matter of an error brought about by taking  $C$  as zero. The value of  $C$  of the wall 3 is presumed larger than the value of the wall 1, therefore it is considered that from equation (28)  $T_{w3}$  is assumed slightly higher than that in Fig. 7 and  $T_{w1}$  is lower than in Fig. 7. In other words, the effect of the optical thickness  $\tau_d$  is to appear smaller than in Fig. 7, although the difference is small. Consideration is extended to the effect of wall emissivity  $\epsilon$ . For smaller  $\epsilon$ , the effect of the optical thickness  $\tau_d$  becomes smaller because the difference between  $T_{w3}$  and  $T_{w1}$  gets larger and the effect of radiation becomes smaller. Figure 8 shows an instance in the case of turbulent flow. The effect of wall radiation will not appear when  $\tau_d$  is above 2 as well as in the case of laminar flow, and the effect of  $\tau_d$  is smaller as the heat transfer by radiation is smaller compared with that by convection than in the case of laminar flow.

4.2. Counter flow heat exchangers

Figures 9 and 10 show instances of the results obtained for the case when the inlet temperature of high temperature side gas  $T_{m2}(l)$  is twice the inlet temperature of low temperature side gas  $T_{m1}(0) = 1$ , assuming fundamental equations (17) and (18) as  $C$

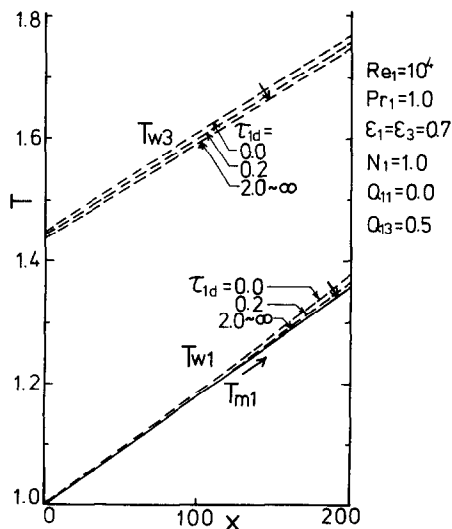


FIG. 8. Case of constant wall heat flux in one flow duct (turbulent flow).

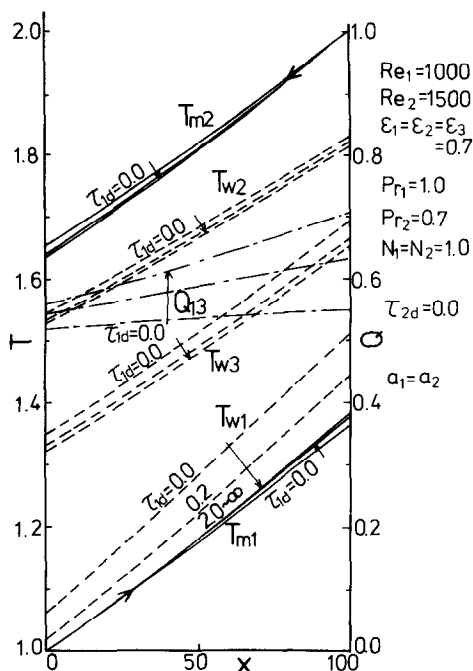


FIG. 9. Case of counterflow heat exchanger (laminar flow).

$= 0$ . In the figures, the heat transferred between the gases  $Q_{13}$  is shown together with temperatures of the gases and the walls. Figure 9 shows the case of the laminar flow and Fig. 10 the turbulent flow, both of which are, not taking into developing regions, of such a case that a radiating gas of optical thickness  $\tau_{1d}$  flows through the low temperature duct and a non-radiating gas such as helium ( $\tau_{2d} = 0$ ) through the high temperature duct.

As seen in Fig. 9, radiation of the intermediate wall does not reach the low temperature wall when  $\tau_{1d}$  is

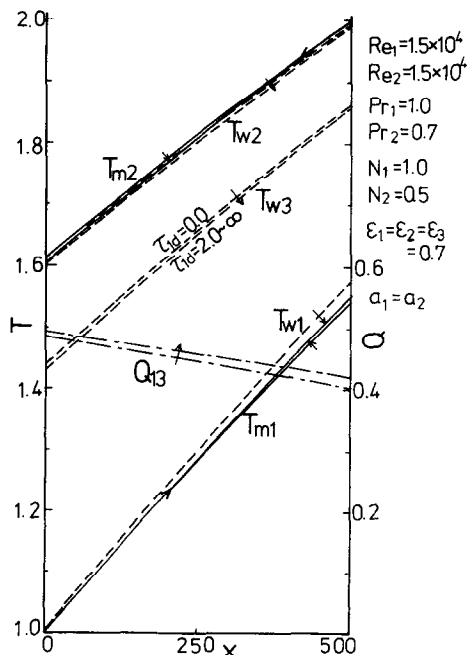


FIG. 10. Case of counterflow heat exchanger (turbulent flow).

above 2 the same as with the one flow duct. Temperature efficiency of heat exchanger is increased, as the rate of the gas temperature  $T_{m1}$  rise in the low temperature side increases although very slightly when  $\tau_{1d}$  becomes large and the heat transferred through the intermediate wall also increases. It is seen that the gas temperature  $T_{m2}$  at the high temperature side as well as the wall temperature  $T_{w2}$  are under the effect of optical thickness  $\tau_{1d}$  of the low temperature duct gas.

In Fig. 10, the radiation parameter in the high temperature duct  $N_2$  is smaller than  $N_1$ , taking the physical properties of the gases into account. Radiation effect is not clear compared with that in Fig. 9 because of a turbulent flow, but has the same tendency.

In the above calculation, the temperature dependence of absorption coefficient was not taken into consideration, but according to the calculation method mentioned above, it will be possible to take the temperature dependence of  $\kappa$  into consideration.

### 5. CONCLUSION

When grey radiating gases flow in ducts consisting of parallel flat plates, and for the field where forced convection radiation co-exist, theoretical calculations on heat transfer performance have been made in the cases of constant heat flux in one duct and counter flow heat exchangers of two flow ducts, to obtain the following results.

(1) When the one-dimensional radiation approximation is considered, the reference temperature  $T_r$  on radiation of gas is introduced and the relation with the mixed mean temperature  $T_m$  is obtained. It is clear that if  $T_r$  is taken to be equal to  $T_m$ , there will be little error in the result, particularly in the case of a turbulent flow.

(2) For a flow of radiating gas, the error caused by taking the heat transfer coefficient of forced convection equal to the case without radiation is negligibly small in practical use.

(3) The radiation effect when the heat flux is given only from the one side wall in the one flow duct is investigated; the radiation from the high temperature wall would not reach the low temperature wall if the optical thickness of radiative medium is above 2 and the radiation effect between the walls would decrease.

(4) In the counter flow heat exchanger consisting of two ducts, with an increase of optical thickness of radiative gas in the low temperature duct, the radiation effect between the solid walls decreases, and though very slightly, the temperature efficiency of the heat exchanger would rise.

### REFERENCES

1. Y. Mori, K. Hijikata and Y. Yamada, Radiation effects on heat transfer in the reactor core heat exchangers of an HTGR, *J. Heat Transfer* **97**, 400 (1975).
2. Y. Mori, T. Taira and K. Watanabe, Radiation effects on heat transfer in heat exchangers—1. *Trans. Japan Soc. Mech. Engrs* **43**, 2670 (1977).
3. Y. Kurosaki, Heat transfer by radiation and other transport mechanisms—2. *Trans. Japan Soc. Mech. Engrs* **35**, 2099 (1969).
4. S. Hasegawa, R. Echigo and Y. Tani, Simultaneous radiative and convective heat transfer of laminar flow between parallel flat plates with uniform heat fluxes, *Trans. Japan Soc. Mech. Engrs* **39**, 1628 (1973).
5. R. Echigo, S. Hasegawa and K. Kamiuto, Composite heat transfer in a pipe with thermal radiation of two-dimensional transfer (relating to the temperature rise in flowing medium upstream from heating section), *Trans. Japan Soc. Mech. Engrs* **40**, 1340 (1974).
6. R. Viskanta, Interaction of heat transfer by conduction, convection, and radiation in a radiating fluid, *J. Heat Transfer* **85**, 318 (1963).
7. B. A. Finlayson, *The Method for Weighted Residuals and Variational Principles*. Academic Press, New York (1972).
8. W. M. Rohsenow and J. P. Harnett, *Handbook of Heat Transfer*, pp. 7-73, 7-74, 7-92. McGraw-Hill, New York (1973).

### EFFET DU RAYONNEMENT SUR LES PERFORMANCES DES ECHANGEURS RADIATIFS A GAZ, AUX HAUTES TEMPERATURES

**Résumé**—Les fluides dans les échangeurs de chaleur dans les réacteurs à gaz à haute température (HTGR) sont considérés comme rayonnants, tels que la vapeur d'eau, CO et autres. On étudie théoriquement les effets du rayonnement sur les performances des échangeurs qui utilisent des gaz rayonnants du fait des températures élevées. Une méthode pour obtenir des solutions approchées est proposée pour être appliquée à de nombreux problèmes pratiques dans une large gamme de température, de pression et d'absorptivité de gaz. Les performances thermiques du cas à flux thermique constant pour un canal et du cas des échangeurs à contre-courant à deux canaux sont calculées pour donner des informations fondamentales sur les échangeurs à hélium et à vapeur d'eau.

### STRAHLUNGSEINFLÜSSE AUF DIE LEISTUNG VON WÄRMEAUSTAUSCHERN FÜR STRAHLENDE GASE BEI HOHEN TEMPERATUREN

**Zusammenfassung**—Die Arbeitsmittel in Wärmetauschern, die man bei einem gasgekühlten Hochtemperaturreaktor anwendet, werden als strahlende Gase betrachtet, wie z. B. Dampf, Kohlenmonoxid, usw. In dieser Arbeit werden die Strahlungseinflüsse auf die Leistungen von Wärmetauschern theoretisch untersucht, in denen strahlendes Gas, wie z. B. Dampf von Hoch-Temperatur-Helium aufgeheizt wird. Es wird eine Methode vorgeschlagen, um zu einer Näherungslösung zu kommen, die für viele praktische Probleme in einem weiten Bereich von Temperatur, Druck und Gasabsorption anwendbar ist. Weiterhin werden Wärmeübertragungsleistungen bei konstanter Wärmestromdichte für ein Rohr und für Gegenstrom-Wärmetauscher mit 2 Rohren berechnet, um grundlegende Informationen über Wärmetauscher für heißes Helium und Dampf zu erhalten.

### ВЛИЯНИЕ ИЗЛУЧЕНИЯ НА РАБОЧИЕ ХАРАКТЕРИСТИКИ РАДИАЦИОННЫХ ГАЗОВЫХ ТЕПЛООБМЕННИКОВ ПРИ ВЫСОКИХ ТЕМПЕРАТУРАХ

**Аннотация** — Рабочие жидкости, такие как водяной пар, СО и др., используемые в теплообменниках высокотемпературного реактора с газовым охлаждением, рассматриваются как газы, выделяющие тепло излучением. Теоретически исследуется влияние излучения на рабочие характеристики теплообменников, в которых тепло передается от сильно нагретого гелия к водяному пару. Предложен метод получения приближенных решений, который можно использовать для решения многих практических задач в широком диапазоне температур, давлений, поглощательных способностей газа и т. д. Проведен расчет характеристик теплопереноса в случаях постоянной плотности теплового потока в одноканальном теплообменнике и противоточных двухканальных теплообменниках с целью получения основных параметров теплообменников, работающих на горячем гелии и водяном паре.